the plant journal

SEB SOCIETY FOR EXPERIMENTAL BIOLOGY

The Plant Journal (2020) **102,** 977–991 doi: 10.1111/tpj.14681

Dual function of HYPONASTIC LEAVES 1 during early skotomorphogenic growth in Arabidopsis

Juan Manuel Sacnun, Roberta Crespo, Javier Palatnik, Rodolfo Rasia and Nahuel González-Schain*
Instituto de Biología Molecular y Celular de Rosario, CONICET, Facultad de Ciencias Bioquímicas y Farmacéuticas, Universidad Nacional de Rosario, Rosario, Argentina

Received 22 August 2019; accepted 3 January 2020; published online 10 January 2020.
*For correspondence (e-mail schain@ibr-conicet.gov.ar).

SUMMARY

Seeds germinating underground display a specific developmental programme, termed skotomorphogenesis, to ensure survival of the emerging seedlings until they reach the light. They rapidly elongate the hypocotyl and maintain the cotyledons closed, forming a hook with the hypocotyl in order to protect apical meristematic cells from mechanical damage. Such crucial events for the fate of the seedling are tightly regulated and although some transcriptional regulators and phytohormones are known to be implicated in this regulation, we are still far from a complete understanding of these biological processes. Our work provides information on the diverse roles in skotomorphogenesis of the core components of microRNA biogenesis in Arabidopsis, HYL1, DCL1, and SE. We show that hypocotyl elongation is promoted by all these components, probably through the action of specific miRNAs. Hook development also depends on these proteins however, remarkably, HYL1 exerts its role in an opposite way to DCL1 and SE. Interestingly, we found that a specific HYL1 domain involved in protein–protein interaction is required for this function. Genetic evidences also point to the phosphorylation status of HYL1 as important for this function. We propose that HYL1 help maintain the hook closed during early skotomorphogenesis in a microprocessor-independent manner by repressing the activity of HY5, the transcriptional master regulator that triggers light responses. This work uncovers a previously unnoticed link between components of the miRNA biogenesis machinery, the skotomorphogenic growth, and hook development in Arabidopsis.

Keywords: *Arabidopsis thaliana*, HYL1, miRNA, microprocessing, skotomorphogenesis, hook unfolding, HY5.

INTRODUCTION

Seeds buried in the soil have evolved a particular developmental programme to grow heterotrophically until the seedling emerges and reaches the light, where it can change its developmental program to autotrophic growth. Thus, growth in darkness, or skotomorphogenesis, is characterized by an exaggerated growth of hypocotyl while cotyledons remain closed, protecting the shoot apical meristem by forming a hook between them and the hypocotyl (Josse and Halliday, 2008). Seed reserves are limited, hence a proper skotomorphogenic growth must be achieved in order to ensure survival of seedlings until they reach the light. A complex network of transcription factors and phytohormones such as ethylene, auxins and gibberellins tightly regulates skotomorphogenic growth once seeds germinate and during the transition to light (Mazzella *et al.*, 2014; Gommers and Monte, 2018). bHLH PHYTOCHROME INTERACTING FACTORS (PIFs) exert their promoting role in darkness and, at the same time, repress photomorphogenesis (Leivar *et al.*, 2008). Conversely, the bZIP transcription factor ELONGATED HYPOCOTYL5 (HY5) acts as a master transcriptional regulator during photomorphogenesis (revised in Gangappa and Botto, 2016). In darkness, HY5 is targeted for degradation by the E3 ubiquitin-ligase CONSTITUTIVE PHOTOMORPHOGENIC1 (COP1) (Osterlund *et al.*, 2000).

MicroRNAs (miRNAs) are a family of small (21–24 nucleotides) RNAs critical for a number of biological processes in eukaryotes. In plants, these small molecules are able to silence specific target genes by base complementarity and cleavage – or translation inhibition – of target mRNAs. miRNAs have a great impact in plant growth, development, and stress-related responses as many of their target genes encode transcription factors and other key regulator proteins. They differ from other families of small RNAs in their biogenesis, which is performed by a

specific protein complex in the nucleus. DICER LIKE 1 (DCL1), SERRATE (SE) and HYPONASTIC LEAVES1 (HYL1) are considered to be the core complex that processes primary messengers of miRNAs (pri-miRNA) into miRNAs. While DCL1 carry out endonucleolytic cleavages of miRNA precursors, SE and HYL1 act as adaptors to ensure the efficiency and accuracy of this process (Kurihara *et al.*, 2006; Dong *et al.*, 2008; Iwata *et al.*, 2013). Mutant plants in those proteins display an accumulation of pri-miRNAs and low levels of many families of miRNAs, as well as many developmental and growth defects (Lu and Fedoroff, 2000; Prigge and Wagner, 2001; Schauer *et al.*, 2002; Vazquez *et al.*, 2004; Yang *et al.*, 2006).

HYL1 comprises two double-stranded RNA-binding domains (dsRBD1 and dsRBD2) in its N-terminus end and six consecutive 28 residue repeats of unknown function in its C-terminus. These repeats seem to be expendable for its function, as a truncated version of HYL1 with only the dsRBD1-dsRBD2 region is able to complement *hyl1-2* mutant in leaves (Wu *et al.*, 2007). While dsRBD1 is involved in binding to miRNA precursors (Rasia *et al.*, 2010; Yang *et al.*, 2010; Burdisso *et al.*, 2014), dsRBD2 participates in protein–protein interaction with DCL1 (Kurihara *et al.*, 2006; Qin *et al.*, 2010), SE (Machida *et al.*, 2011), and in homodimerization (Yang *et al.*, 2010; Yang *et al.*, 2014). HYL1 is also regulated post-translationally by dephosphorylation of serine residues by C-TERMINAL DOMAIN PHOSPHATASE-LIKE 1 (CPL1, (Manavella *et al.*, 2012)), protein phosphatase 4 and SMEK complex (Su *et al.*, 2017), and is a potential substrate of phosphorylation by MPK3 and SnRK2 kinases (Raghuram *et al.*, 2015; Yan *et al.*, 2017). Also, its level depends on the proteolytic degradation by an unknown protease after a transition from light to dark conditions in adult plants (Cho *et al.*, 2014). A recent report has shown that these post-translational modifications, particularly the phosphorylation status of HYL1, are important to quickly respond to light after periods of light deprivation (Achkar *et al.*, 2018). The developmental defects displayed in *HYL1* mutant plants have evidenced the many biological processes in which the microprocessor is involved, such as leaf curvature, elongation of stamen filaments that affect fertility, or altered responses to phytohormones, among others (Lu and Fedoroff, 2000).

Some recent studies have suggested a role for HYL1 and other components of the microprocessor in early light-grown seedling development and in dark-to-light transition (Cho *et al.*, 2014; Tsai *et al.*, 2014; Sun *et al.*, 2018). However, the relevance of miRNA biogenesis components during skotomorphogenic growth is still poorly understood. Here we show that the microRNA pathway is required during Arabidopsis skotomorphogenic growth to ensure proper development of hypocotyls and apical hooks until seedlings reach the light. Our results indicate different roles of core proteins belonging to the microprocessor complex in different tissues during skotomorphogenesis. We found that DCL1, HYL1, and SE promote hypocotyl elongation. As expected, mutants in these genes have similar phenotypes as they act together in miRNA biogenesis. However, we found a more complex scenario in hook development. While DCL1 and SE promote hook unfolding, HYL1 repressed it. The specific role of HYL1 in the repression of hook development seems to operate through protein–protein interactions rather than through miRNA biogenesis. This work, together with recent findings on the phosphorylation status of HYL1 in darkness (Achkar *et al.*, 2018), point to phosphorylated HYL1, which is inactive in miRNA biogenesis, having a function during normal hook development. We propose an alternative regulatory layer linking HYL1 to HY5 during skotomorphogenic growth.

RESULTS

HYL1 is necessary for a proper skotomorphogenic growth

The initial characterization of *HYL1* showed that mutant seedlings develop shorter hypocotyls than wild-type plants (Lu and Fedoroff, 2000; Tsai *et al.*, 2014). However, no further analysis was carried out to understand the role of HYL1 on skotomorphogenic development. We tested the main characteristic phenotypes of seedlings grown in darkness, that is hypocotyl elongation and hook development, in time-course experiments from 2 to 4 days in darkness (dD). *hyl1-2* mutants have consistently shorter hypocotyls than wild-type (WT) seedlings at all time points analyzed (Figure 1a,b). These differences cannot be attributed to a delay in germination of *hyl1-2* seeds as this is not affected (Figure S1). The requirement of HYL1 to elongate the hypocotyl properly seems to be specific for dark conditions since this mutant did not show any significant differences with WT at early stages in light conditions in long day (LD) conditions (Figure S2a,b). Lu and Fedoroff described a reduced hypocotyl elongation rate of *hyl1* mutants grown in Murashige and Skoog (MS) medium supplemented with 1% sucrose (MS1) in light conditions (Lu and Fedoroff, 2000), but did not specify the age of the seedlings measured. We then tested our half-strength MS (0.5MS) with MS1 conditions on *hyl1-2* mutants growing in LD. Results showed that hypocotyl length of *hyl1-2* mutants is indistinguishable from WT in light, in both growing conditions, at least in early development where this work is focused (Figure S2c). Conversely, the apical hook is significantly more open in *hyl1-2* than in WT seedlings during skotomorphogenic growth (Figure 1a,c). Overall, plants lacking HYL1 seem to develop a partial photomorphogenic growth in darkness. As phenotypic differences can be seen at 2 dD and both hypocotyl elongation and hook opening rates remain relatively unchanged at later time points, we hypothesize that the presence of HYL1 is more relevant at early than late stages during skotomorphogenesis.

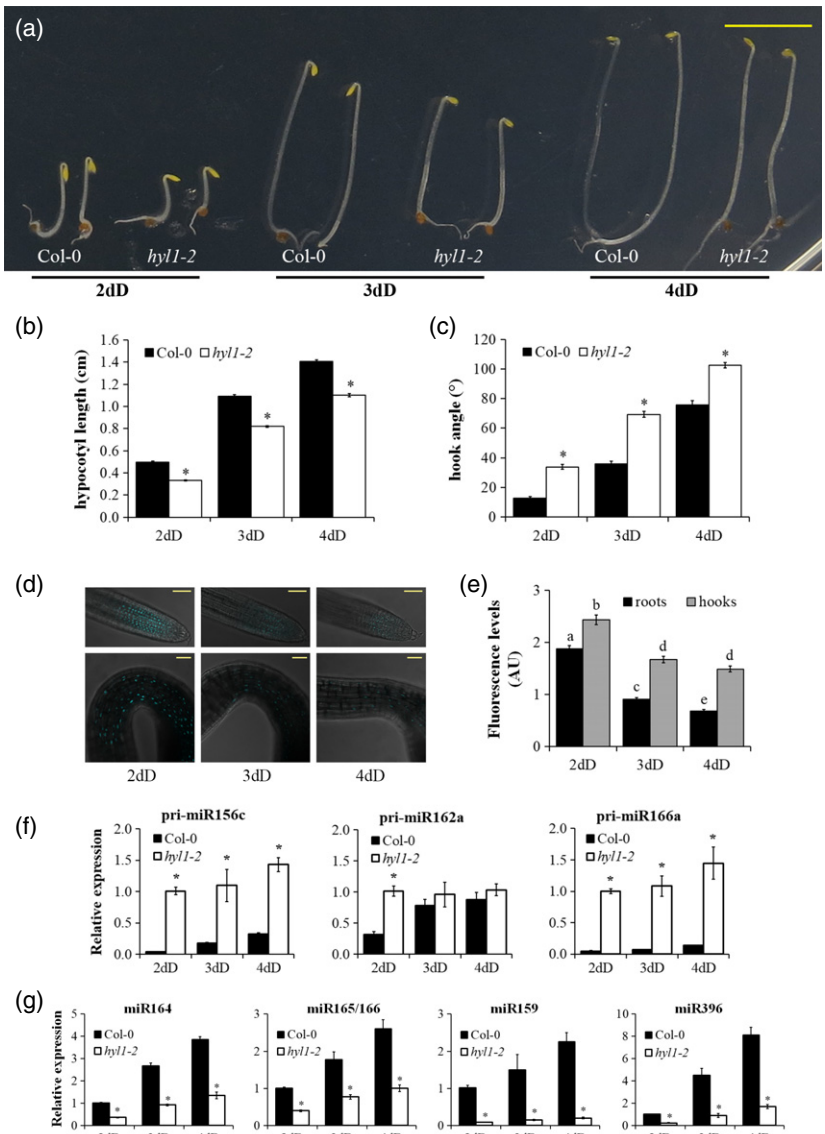

Figure 1. HYL1 is required for early skotomorphogenic growth. (a) Representative *hyl1-2* and control (Col-0) seedlings grown in darkness. dD indicates days in the dark. (b) Hypocotyl length and (c) hook angle measurements of *hyl1-2* and Col-0 dark-grown seedlings at the indicated time points. Data are reported as mean ± SEM of at least 40 seedlings from five biological replicas. (d) Representative confocal fluorescence images of roots (upper panels) and hooks (lower panels) from dark-grown pHYL1::HYL1-CFP *hyl1-2* seedlings at the indicated time points. (e) Integrated fluorescence intensity of root and hook nuclei from dark-grown pHYL1::HYL1-CFP *hyl1-2* seedlings at the indicated time points. Data are reported as mean ± SEM of at least 70 nuclei from two biological replicas. AU, Arbitrary units. (f) and (g) qRT-PCR and stem–loop qRT-PCR analysis, respectively, of *hyl1-2* and Col-0 dark-grown seedlings at the indicated time points. Expression levels of pri-miRNA (f) or miRNAs (g) were normalized to the *PP2AA3* housekeeping gene and expressed relative to the *hyl1-2* (f) or Col-0 (g) 2 dD value set at unity. Means ± SEM are shown from technical triplicates and two biological replicas. Asterisks in (b), (c), (f) and (g) indicate statistically different mean values compared with their corresponding wild-type ($P < 0.05$). Statistically significant differences between groups in (e) are indicated by different letters (ANOVA, $P < 0.05$). Bar in (a) represents 5 mm and in (d) represents 50 μm.

To study the localization of HYL1 during skotomorphogenic growth we generated *hyl1-2* plants expressing HYL1-cyan fluorescent protein (CFP) under the control of its own promoter [pHYL1::HYL1-CFP; (Fang and Spector, 2007)]. Several transgenic lines expressing the fusion protein were obtained, and the difference in expression levels between lines was evaluated by measuring fluorescence intensities of nuclei in roots (Figure S3a,b). Despite the differences in expression levels, all pHYL1::HYL1-CFP lines were able to complement the phenotypes displayed by *hyl1-2* mutants during skotomorphogenesis (Figure S3c,d) as well as in adult plants (Figure S3e). HYL1-CFP fluorescence was detected in nuclei of roots, hooks (Figures 1d, S3b, and S4a), hypocotyls, and cotyledons during skotomorphogenesis. Some seedlings displayed diffuse fluorescence signals in roots (Figure S4b) and other tissues with no clear localization. We chose homozygous lines 10 and 15 with *c.* five-fold level differences in HYL1 expression, as quantified by fluorescence (Figure S3a) for further studies in order to address quantitative aspects of HYL1 localization by confocal fluorescence microscopy. First, we quantified the number of seedlings with discrete nuclear or diffuse localization in different tissues of both lines. HYL1–CFP turn from nuclear to diffuse localization in roots and hypocotyls as the skotomorphogenesis progresses in most seedlings. In contrast, HYL1–CFP remains nuclear in hooks at all three time points tested in both lines in almost all seedlings (Table S1). We then quantified fluorescence intensities of nuclei from those seedlings with discrete nuclear localization. Figure 1(d,e) shows that the level of HYL1-CFP decreases in roots as skotomorphogenesis progresses, while fluorescence intensities remained constant in hooks after an initial drop from 2 dD to 3 dD.

In summary, our results suggest that HYL1 is present during early stages of development in darkness and is degraded in most tissues as skotomorphogenesis progresses. The persistence of HYL1 levels in hooks could indicate that proteolytic regulation is not taking place in that tissue and that the protein could have a role in the repression of hook opening.

miRNA biogenesis is active during skotomorphogenesis

HYL1 is a key adaptor within the dicing complex to precisely and efficiently generate microRNAs (miRNAs) from their primary RNA precursors [pri-miRNAs; (Kurihara *et al.*, 2006)]. Whether this machinery is ubiquitously active or time and developmentally regulated is not known, and there is currently no information on whether miRNA biogenesis is active during skotomorphogenesis. With a few exceptions (Wang *et al.*, 2018), plants with mutations in miRNA biogenesis proteins fail to generate miRNAs and accumulate pri-miRNAs. We tested the expression levels of nine pri-miRNAs, 156b, 156c, 156d, 159b, 162a, 164c, 166a, 166b, and 171b in *hyl1-2* and Col-0 dark-grown seedlings. All nine precursors accumulated in the mutant at higher levels than in controls at 2 dD (Figures 1f and S5). Moreover, this over-accumulation persisted even at 4 dD for most of them although with smaller differences. To test whether this accumulation of pri-miRNAs in *hyl1-2* is due to a deficient microprocessor activity we checked the abundance of several miRNAs by stem–loop qPCR. Compared with WT seedlings, a very small amount of miRNAs is produced in *HYL1* mutant seedlings in darkness (Figure 1g), indicating that HYL1 activity, through the biogenesis of miRNAs, is important during skotomorphogenesis.

We then asked if HYL1 activity changed in different tissues from dark-grown seedlings. We dissected roots and hooks from 2 dD-grown *hyl1-2* and Col-0 seedlings, purified RNA from two independent experiments and tested the expression levels of several pri-miRNAs and miRNAs by qPCR as described above. Results showed an over-accumulation of pri-miRNAs in *hyl1-2* hooks (Figure S6a), that is in line with the results obtained in whole seedlings (Figures 1f and S5). In contrast, dissected roots obtained from the same *hyl1-2* samples displayed lower accumulation of pri-miRNA-156c and −159b compared with hooks, and even no significant differences were found for pri-miRNA-162a and −166a (Figure S6a). These results suggested that HYL1 activity is more important in hooks than in roots during early skotomorphogenesis. The pattern of miRNA accumulation in both tissues from *hyl1-2* and Col-0 (Figure S6b) showed a similar trend as in whole seedlings (Figure 1g).

Taken together, our results clearly showed that miRNA processing is taking place during early skotomorphogenic growth and that the activity of the miRNA biogenesis pathway appears to be tissue dependent.

Other components of the microRNA pathway are involved in skotomorphogenesis

As HYL1 is actively participating in the skotomorphogenic growth, and no specific role beside microRNA biogenesis was found for this protein until now, we expected to find a similar role for other components of the microRNA pathway. DCL1 and SE form together with HYL1 the core component of the microRNA biogenesis machinery. We therefore tested whether *se-1* and *dcl1-100* mutants displayed similar phenotypes as *hyl1-2* in dark-grown seedlings. Mutants in *SE* exhibited significantly shorter hypocotyls than WT during skotomorphogenesis (Figure 2a,b). Unexpectedly, hook angle is less open in *se-1* at all time points tested (Figure 2a,c), showing a phenotype opposite to *hyl1-2*. We also tested the behaviour of light-grown *se-1* mutants. Although significant differences were found in hypocotyl elongation between *se-1* and WT at 3 days in LD these are rather small and probably with low biological impact (Figure S7a,b). This suggests that, as in *HYL1* mutants, the role of SE in early development is more relevant during skotomorphogenesis. In order to study the localization of SE protein in dark-grown seedlings we generated pSE::YFP-SE lines in *se-1* background and checked fluorescence by confocal microscopy. Images obtained from several independent lines grown at 3 dD showed localization of YFP-SE in nucleoplasm from all tested tissues: hooks, hypocotyls, roots and cotyledons (Figure 2d). Given that SE is present during skotomorphogenesis and the phenotypes observed in *se-1*, we next tested whether miRNA biogenesis is impaired in dark-grown mutant seedlings. We tested the expression of nine pri-miRNAs in *se*-1 and WT seedlings grown 2 dD and 4 dD by qPCR. Results showed an over-accumulation of all pri-miRNAs tested in *se-1* (Figures 2e and S5) indicating that miRNA biogenesis is active during skotomorphogenesis, as was suggested previously from *hyl1-2* experiments. Similar to that observed in *hyl1-2* mutants, miRNAs accumulation is also impaired in *se-1* during skotomorphogenesis (Figure 2f). We tested for phenotypic alterations in dark-grown *DCL1* mutants as well, by using the hypomorphic allele *dcl1-100*. As homozygous mutants are sterile, we carried out experiments in darkness using *dcl1-100* heterozygous lines and its WT siblings as controls. Dark-grown homozygous *dcl1-100* seedlings are easily recognized in a segregating population in the plates after an additional 4 days growth in light (Figure S8a,b). Their cotyledons are hardly completely opened, as in *hyl1-2* mutants (Figure S2a), and segregation analyses correlated well with genotypes of these seedlings (Table S2). Hypocotyl elongation rate is significantly slower in *dcl1-100* compared with the rest of heterozygous and WT segregating seedlings, as well as with WT siblings grown in parallel (Figure S8a,c), thus resembling

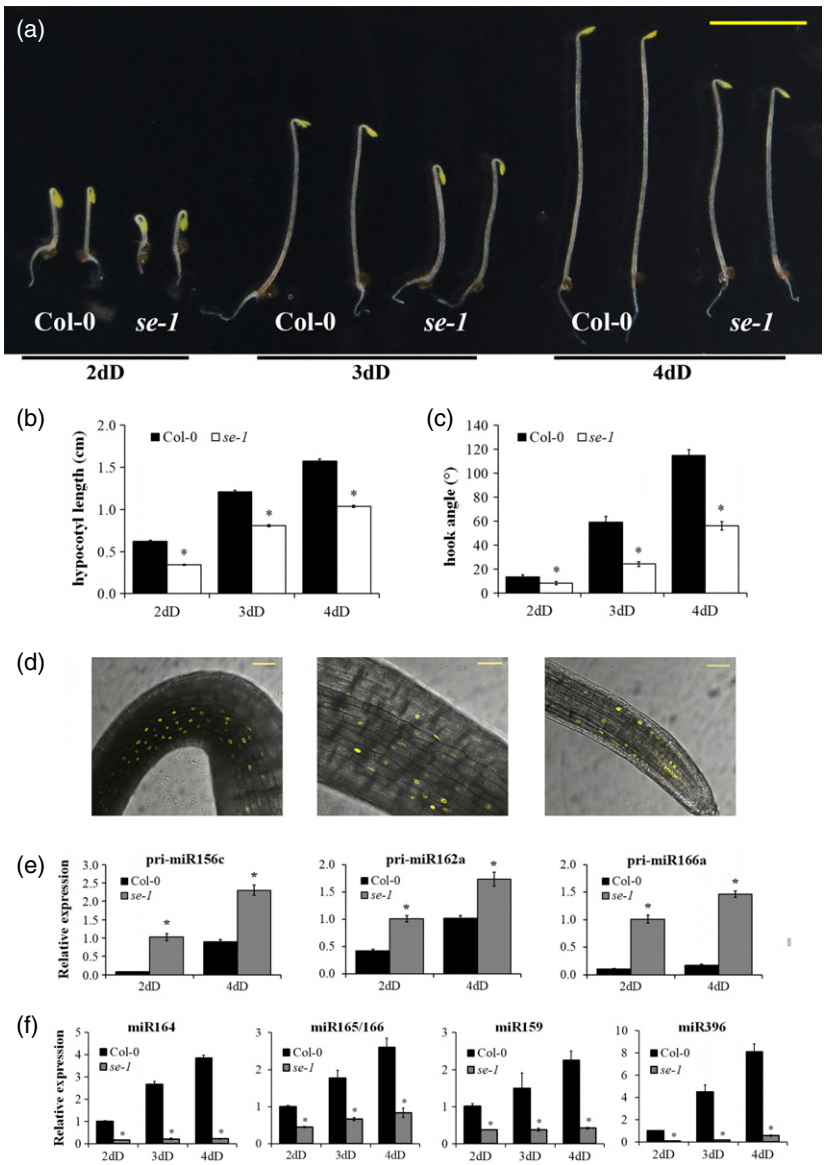

Figure 2. SE participation in skotomorphogenesis. (a) Representative *se-1* and control (Col-0) seedlings grown in darkness are shown. dD indicates days in the dark. (b) Hypocotyl length and (c) hook angle measurements of *se-1* and Col-0 dark-grown seedlings at the indicated time points. Data are presented as mean ± SEM of at least 40 seedlings from two biological replicas. (d) Representative confocal fluorescence images of hooks, hypocotyls, and roots from 3-days dark-grown T1 pSE::YFP-SE seedlings. (e, f) qRT-PCR and stem–loop qRT-PCR analysis, respectively, of *se-1* and Col-0 dark-grown seedlings at the indicated time points. Expression levels of pri-miRNAs (e) or miRNAs (f) were normalized to the *PP2AA3* housekeeping gene and expressed relative to the *se-1* (e) or Col-0 (f) 2 dD value set at unity. Means ± SEM are shown from technical triplicates and two biological replicas. Asterisks in (b), (c), (e) and (f) indicate statistically different mean values compared with their corresponding wild-type ($P < 0.05$). Bar in (a) represents 5 mm and in (d) represents 50 μm.

hyl1-2 phenotypes. In contrast, hook angle is less open in *dcl1-100* at all time points tested (Figure S8a,d), this phenotype being the same as the *SE* mutants and opposite to *hyl1-2*. We also tested if other components of miRNA pathway are important for hook development: the methyltransferase *HEN1*, which protects mature miRNAs by methylation (Yu *et al.*, 2005); the nuclear exportin *HASTY*, involved in the nucleocytoplasmic transport of miRNAs (Park *et al.*, 2005); and *ARGONAUTE1* (Baumberger and Baulcombe, 2005), the RNA slicer in the RNA-induced silencing complex (RISC). The hypomorphic allele *ago1-27* displays a delay in hook opening although much weaker than in *se-1* or *dcl1-100* (Figure S9a). *hen1-8* mutant displays a weak phenotype that increases during the days in darkness. On its side, hook unfolding in *hst-15* resembles the *hyl1-2* mutant (Figure S9a). Its noteworthy that *hst* mutants exhibited hyponastic leaves in adult plants (Bollman *et al.*, 2003; Figure S9b), much like *hyl1-2* mutants.

Taken together, our results demonstrate that miRNA biogenesis is required to rapidly elongate the hypocotyl in order to seek light during skotomorphogenesis. Hook development is also influenced by proteins belonging to the miRNA pathway, but our results obtained from mutants of the core components of the miRNA biogenesis identify a specific role for HYL1 that acts in an opposite way to DCL1 and SE. This led us to study the role of HYL1 on skotomorphogenesis in more detail.

HYL1 dsRBD1 is required for miRNA biogenesis but not for hook development during skotomorphogenesis

HYL1 comprises two double-stranded RNA-binding domains (dsRBDs) in its N-terminal end, a nuclear

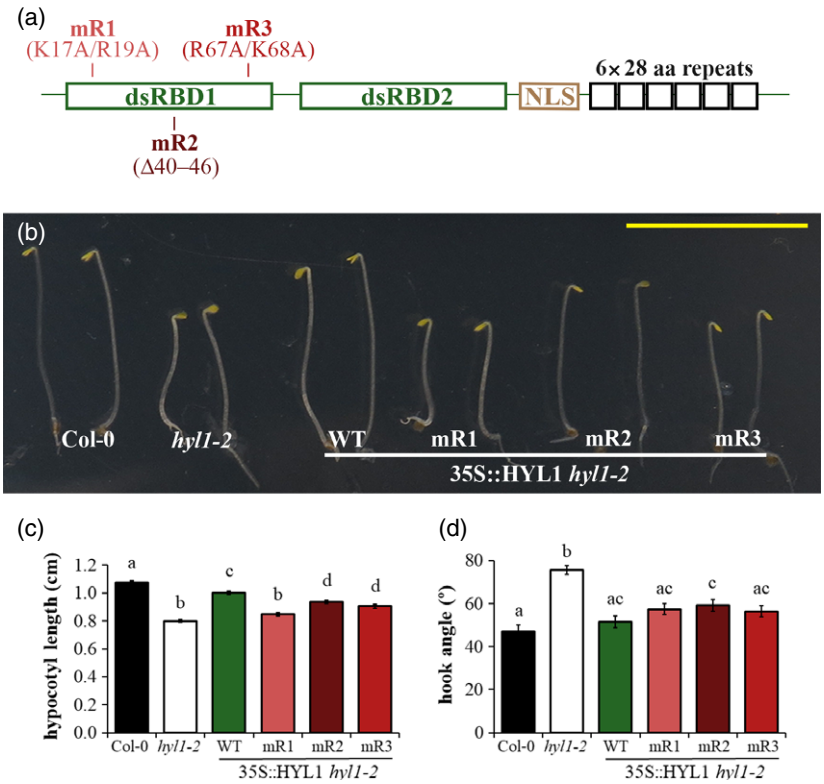

Figure 3. The dsRBD1 domain of HYL1 is not involved in hook unfolding regulation in darkness. (a) Schematic view of HYL1 protein. The two double-stranded RNA-binding domains (dsRBD), nuclear localization signal (NLS) and repetitions at the C- terminal end are indicated. mR1, mR2 and mR3 mutant versions in dsRBD1 (Burdisso *et al.*, 2014) are also indicated. (b) Representative *hyl1-2*, control (Col-0) and plants expressing wild-type or mutant versions of HYL1 dsRBD1 in *hyl1-2* background from 3-days dark-grown seedlings are shown. dD indicates days in the dark. (c) Hypocotyl length and (d) hook angle measurements of the plants shown in (b). Data are presented as mean ± SEM of at least 40 seedlings from two biological replicas. Statistically significant differences between groups in (c) and (d) are indicated by different letters (ANOVA, $P < 0.05$). Bar in (b) represents 5 mm.

localization signal and six repetitions of 28 amino acids in its C-terminal region (Figure 3a). In order to dissect the role of particular domains of HYL1 during skotomorphogenesis, we tested three mutant transgenic lines in dsRBD1. We have previously demonstrated that mutations in dsRNA binding region 1 are most detrimental to the miRNA processing activity of HYL1 *in vivo*, whereas mutations in regions 2 and 3 affect its activity to a lesser extent (Burdisso *et al.*, 2014). Overexpression of HYL1 mutants in region 1 of dsRBD1 (mR1: K17A/R19A) did not complement *hyl1-2* hypocotyl elongation, while a seven amino acid deletion Δ40-46 in region 2 (mR2) and region 3 mutants (mR3: R67A/K68A) only partially complemented the hypocotyl elongation (Figures 3b,c and S10). The requirement of HYL1 dsRBD1 in hypocotyl elongation goes in line with its role in miRNA biogenesis and function in leaf development (Burdisso *et al.*, 2014). Surprisingly, all mR1, mR2 and mR3 mutants almost fully complemented hook phenotypes in *hyl1-2* (Figure 3b,d), indicating that HYL1 dsRBD1 does not participate in the regulation of hook development during skotomorphogenesis. We observed the same hook development in 35S::HYL1 (Figure 3b,d) as in pHYL1::HYL1-CFP complemented plants (Figure S3), meaning that hook phenotype complementation does not depend on HYL1 levels. We previously observed that both adult phenotypes and miRNA processing efficiency are also independent of HYL1 expression levels in several transgenic lines tested (Burdisso *et al.*, 2014). These results also hinted that the participation of HYL1 in hook development is independent of its role in miRNA biogenesis, as pri-miRNA binding by HYL1 is dominated by dsRBD1 (Qin *et al.*, 2010; Rasia *et al.*, 2010; Burdisso *et al.*, 2014).

Hook unfolding is repressed in mutant lines that affect the phosphorylation status of HYL1

The activity of HYL1 is regulated by phosphorylation in specific serine residues. It was shown that phosphorylated HYL1 displayed a reduced activity and that recruitment to the microprocessor complex is impaired leading to defects in miRNA processing and accumulation (Manavella *et al.*, 2012). In order to verify if phosphorylation regulates HYL1 activity in skotomorphogenesis as well, we analyzed the behaviour of mutants that modify the phosphorylation state of HYL1. C-terminal domain phosphatase-like 1 (CPL1) is the main phosphatase that reactivates HYL1 by dephosphorylation of serine residues (Manavella *et al.*, 2012). We tested a strong (*cpl1-7*) and a mild (*cpl1-3*) allele of *CPL1* mutants during skotomorphogenesis. Both *cpl1* mutants displayed only small differences in hypocotyl elongation (Figure 4a). In contrast, hook unfolding is more repressed in both *cpl1-3* and *cpl1-7* than in WT plants (Figure 4b). The strength of *cpl1-3* and *cpl1-7* phenotypes in hooks correlates well with size defects observed in adult plants (Figure S11). As *CPL* mutants over-accumulate hyperphosphorylated HYL1 (Manavella *et al.*, 2012), their hook phenotypes suggest an active role for

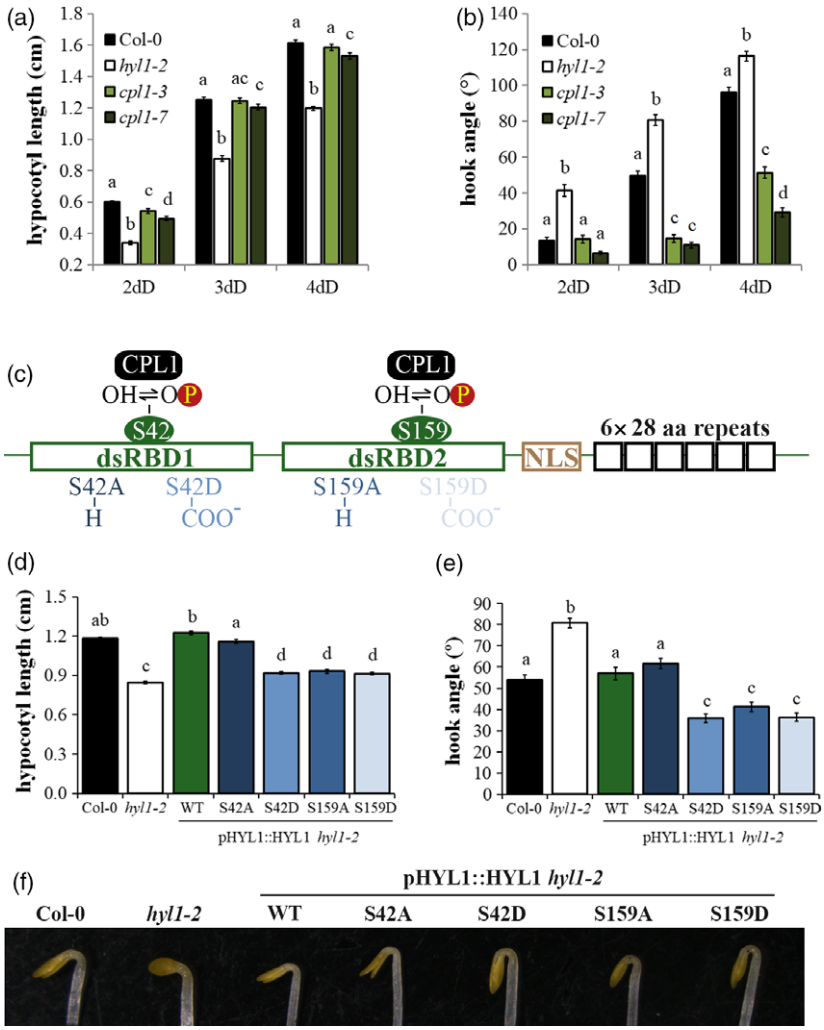

Figure 4. Mutant lines that affect phosphorylation of HYL1 display more closed hooks. (a) Hypocotyl length and (b) hook angle measurements of *hyl1-2*, Col-0 and two mutant alleles of *CPL1* from 2-, 3-, and 4-days dark-grown seedlings. (c) Schematic view of HYL1. Serines 42 and 159 subjected to dephosphorylation by CPL1 are indicated. Hypophosphorylation and hyperphosphorylation mimics (S42A, S159A and S42D, S159D, respectively; Manavella *et al.*, 2012) are also indicated. (d) Hypocotyl length and (e) hook angle measurements of *hyl1-2*, Col-0, and plants expressing wild-type version or hypo/hyperphosphorylation mimics in *hyl1-2* background from 3-days dark-grown seedlings. (f) Representative hooks of transgenic lines from (e). Data are presented as mean ± SEM of at least 40 seedlings from two biological replicas. Statistically significant differences between groups in (a), (b), (d) and (e) are indicated by different letters (ANOVA, $P < 0.05$).

phosphorylated HYL1 in the repression of hook unfolding during darkness. In order to confirm that hook phenotypes in *CPL1* are mediated by HYL1 we made double mutants *hyl1-2 cpl1-3* and *hyl1-2 cpl1-7* and tested them in darkness. Hook unfolding measurements showed *hyl1-2* was epistatic to *cpl1-3* or *cpl1-7* as double mutants phenocopied *hyl1-2* in 2-days dark-grown seedlings (Figure S12). However, this genetic interaction fades away progressively as *hyl1-2 cpl1-3* or *hyl1-2 cpl1-7* resemble WT hooks in 4 dD (Figure S12), in coincidence with the early time-window activity of HYL1 in hooks proposed previously.

Two specific serine residues were described as important for HYL1 phosphorylation mediated regulation: S42 in dsRBD1 and S159 in dsRBD2 (Figure 4c). Mutant versions of S42 or S159 to aspartic acid (S42D or S159D), mimicking constitutive phosphorylation, failed to complement *hyl1-2* defects in leaves, while mutants of seven serines, including S42 and S159, to alanine produced hypophosphorylation mimics of HYL1 that fully restore *hyl1-2* defects (Manavella *et al.*, 2012). We tested whether these mutant lines were able to complement the defects observed in *hyl1-2* during skotomorphogenesis. Hyperphosphorylation mimic versions of HYL1 S42D and S159D were not able to complement the shorter hypocotyls of *hyl1-2* (Figure 4d) nor the leaves phenotypes of adult plants (Figure S13). In contrast, S42D and S159D mimics displayed more closed hooks compared with the WT version or Col-0 at 3 dD (Figure 4e, f). These results further suggest that phosphorylated HYL1 is active in the repression of hook unfolding.

We also tested the hypophosphorylated mutant versions of HYL1, S42A, and S159A. The S42A mutant almost fully complemented both the hypocotyl phenotype and the defects in hook opening of *hyl1-2* (Figure 4d). In line with this, the same mutant restored the curvature in leaves (Figure S13), confirming that the mutation keeps HYL1 active. In contrast, complementation by the S159A mutant in hypocotyls was virtually insignificant (Figure 4d), and the mutant form also leads to more closed hooks (Figure 4e,f). HYL1-S159A shows only partial complementation of the leaf phenotype (Figure S13), suggesting that the activity of

the second dsRBD of HYL1 is partially impaired by the mutation.

HY5 activity and stability is affected in *HYL1* deficient plants during skotomorphogenesis

Given the skotomorphogenic phenotypes displayed in *hyl1-2* and *se-1* mutants, we suspected that dark/light signalling responses could be altered in these mutants. PIFs transcription factors are essential to maintain skotomorphogenic growth by repressing photomorphogenic responses at a transcriptional level in darkness (Leivar *et al.*, 2008). *PIL1* and *XTR7* are targets of PIFs and considered as reporters of PIF transcriptional activity (Leivar *et al.*, 2009; Lorrain *et al.*, 2009). We measured the relative expression of *PIF3*, one of the main components of PIF family with an active role in darkness, and the two targets mentioned above by real-time PCR. Although *PIF3* expression shows statistically significant differences between *hyl1-2* and *se-1* mutants, these are rather small and no differences were detected between both mutants and WT (Figure 5a). These small differences do not seem to reflect a differential transcriptional activity of PIFs between the mutants as no differences in *PIL1* or *XTR7* expression were detected (except for slightly higher levels of *PIL1* expression in *hyl1-2* at 4 dD) (Figure 5a). Taken together, neither the changes in PIFs levels nor their activity in *hyl1-2* or *se-1* mutants justify the partial photomorphogenic growth observed in darkness.

HY5 is a transcription factor that plays a crucial role in photomorphogenic growth promoting the expression of light-regulated genes by binding directly to their promoters (Chattopadhyay *et al.*, 1998; Lee *et al.*, 2007). HY5 is necessary for the transcription of *Chlorophyll A/b Binding protein1* (*CAB1*), *Ribulose bisphosphate carboxylase Small subunit 1A* (*RbcS1A*) and *CHalcone Synthase* (*CHS*) during the dark-to-light transition (Lee *et al.*, 2007). Therefore, we examined the expression levels of these three genes and *HY5* in dark-grown *HYL1* and *SE* mutants by real-time PCR. Statistically significant changes in expression of *HY5*, *CAB1* and *CHS* in *se-1* compared with Col-0 were detected at 2 dD (Figure 5b). Although small, these differences cannot be easily explained as a small induction of *HY5* in *se-1* at 2 dD was not accompanied with an induction of its direct targets tested. Conversely, results consistently show a higher expression level of *HY5* in *hyl1-2* that is in line with the induction of *CAB1*, *RbcS1A* and *CHS* observed at 4 dD (Figure 5b). Taken together, these results suggested that a small fraction of HY5 protein might be active in *hyl1-2* mutants in darkness partially explaining physiological phenotypes observed during skotomorphogenesis.

To test this hypothesis, we made double mutants of *HY5* and *HYL1* or *SE* and measured their hypocotyl elongation and hook unfolding during skotomorphogenesis. *hy5-2* mutants did not show any phenotypic differences compared with WT seedlings, neither in hypocotyl length nor in hook angle, most probably because Constitutive Photomorphogenic 1 (COP1) targets HY5 for proteasome-mediated degradation in the dark (Osterlund *et al.*, 2000). Hypocotyl elongation measurements showed *hyl1-2* or *se-1* were epistatic to *hy5-2*, as both *hyl1-2 hy5-2*, and *se-1 hy5-2* phenocopied *hyl1-2* and *se-1* defects, respectively (Figure 6a). A similar epistatic interaction is shown for *se-1 hy5-2* in hook unfolding in which the closed hook phenotype in *se-1* was not affected by the absence of HY5 (Figure 6b,c). In contrast, we found that the *hy5-2* mutation is able to restore hook phenotypes in the *hyl1-2* mutant seedlings (Figure 6b,c), suggesting again that *HY5* misregulation in the *hyl1-2* mutant was responsible for the hook defects.

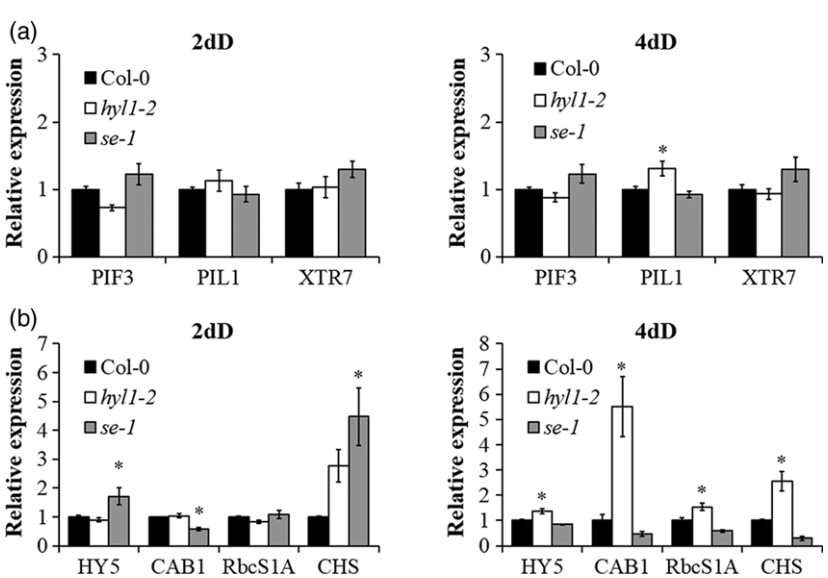

Figure 5. Photomorphogenesis marker genes are repressed by HYL1 in darkness. Expression analysis of (a) *PIF3* and; (b) *HY5*, and their corresponding direct target genes at 2 dD (left) and 4 dD (right). qRT-PCR analysis of *hyl1-2*, *se-1*, and Col-0 dark-grown seedlings at the indicated time points were performed. Expression levels were normalized to the *PP2AA3* housekeeping gene and expressed relative to the Col-0 value set at unity. Means ± SEM are shown from technical triplicates and two biological replicas. Asterisks indicate statistically different mean values compared with their corresponding wild-type ($P < 0.05$).

HY5 levels in darkness were reported to be very low and inactive due to phosphorylation and proteasome-mediated degradation (Hardtke *et al.*, 2000; Osterlund *et al.*, 2000). We measured HY5 levels in pHY5::HY5-YFP *hy5-2* and pHY5::HY5-YFP *hy5-2 hyl1-2* by western blot. HY5 is less abundant in *hyl1-2* background at both time points analyzed (Figure 6d). To test whether HY5 stability in *hyl1-2* depends on the proteolytic activity of the proteasome we performed western blots of protein extracts from MG-132-treated pHY5::HY5-YFP *hy5-2 hyl1-2* seedlings. We found higher amounts of HY5 in MG-132-treated seedlings compared with the mock treatment in four independent experiments (Figure S14). These results suggested that HY5 degradation depends on the proteasome activity in dark-grown *HYL1* deficient lines. To exclude any possible transcriptional effect, we analyzed the expression of *HY5* in both lines by qPCR and we found no significant differences (Figure S15).

Taken together, these results showed that HYL1 plays a role on HY5 activity and stability in skotomorphogenesis.

DISCUSSION

miRNA biogenesis pathway promotes hypocotyl elongation in skotomorphogenesis

Earlier reports have shown that *Arabidopsis thaliana* mutants in *HYL1* and *DCL1* develop shorter hypocotyls than WT plants at specific time points in darkness (Lu and Fedoroff, 2000; Tsai *et al.*, 2014; Sun *et al.*, 2018) but the consistency of this phenotype during skotomorphogenesis has not been previously addressed. Our results indicated that proteins belonging to the core miRNA processing complex promote hypocotyl elongation in darkness, as individual mutants in all three major components of this pathway display shorter hypocotyls. This regulation seems to be specific for skotomorphogenic growth as hypocotyl elongation in diurnal conditions is not affected in *hyl1-2* or *se-1* mutants, as was shown in a very recent report for *HYL1* mutants (Sun *et al.*, 2018). The complementation of hypocotyl elongation of *hyl1-2* mutants with versions of HYL1 bearing alterations in the pri-miRNA interaction

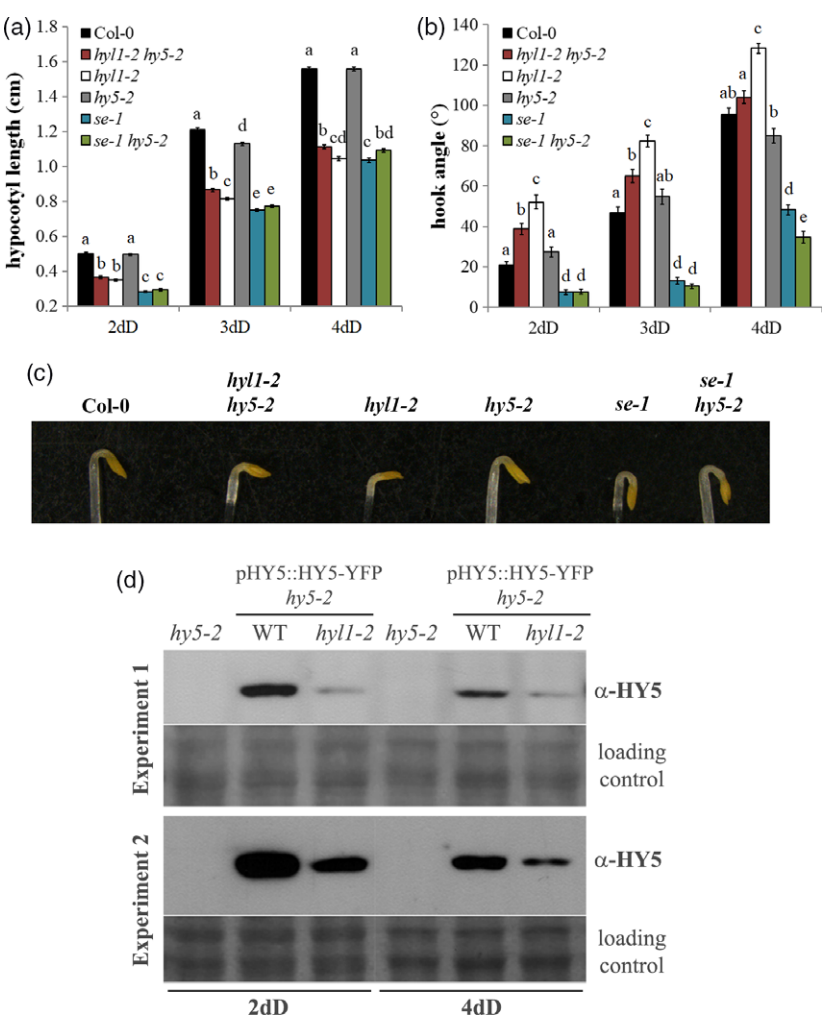

Figure 6. Suppression of *HY5* partially restores hook defects in *HYL1* mutants. (a) Hypocotyl length and (b) hook angle measurements of Col-0, *hyl1-2*, *se-1*, *hy5-2*, and double mutants *hyl1-2 hy5-2* and *se-1 hy5-2* dark-grown seedlings at the indicated time points. (c) Representative hooks of transgenic lines from (b). (d) α-HY5 western blots of 2 and 4-days dark-grown pHY5::HY5-YFP *hy5-2* in *hyl1-2* or Col-0 background seedlings. *hy5-2* mutants were used as negative controls. Ponceau stainings were used as loading controls. Data in (a) and (b) are presented as means ± SEM of at least 40 seedlings from two biological replicas. Statistically significant differences between groups are indicated by different letters (ANOVA, $P < 0.05$).

domain (dsRBD1) parallel the complementation of phenotypes in adult plants. These results revealed that specific miRNAs might be important for cell elongation in hypocotyls. Expression analyses by real-time PCR clearly showed that miRNA biogenesis is actually taking place during skotomorphogenesis. Both miRNA and pri-miRNA levels increased during development in darkness. The more likely explanation for the increase in levels of miRNA precursors is that microprocessing fades out during skotomorphogenesis and that miRNA biogenesis is more relevant at early stages. This agrees with the decay of HYL1 levels through skotomorphogenic development evidenced by quantitative data obtained by fluorescence microscopy. The decreasing relevance of HYL1 during skotomorphogenesis was also evidenced on the dominant phenotypes of *hyl1-2* in double mutants with *cpl1-3* or *cpl1-7*. Hook unfolding is derepressed at early stages but not at later stages, similar to effects observed in *hyl1-2 hy5-2* double mutants. A recent report showed that some miRNAs, like miR319b, miR160b, miR167b, and miR848, act as positive or negative regulators of hypocotyl elongation in seedlings grown under red light, although they are not involved in the same process in darkness (Sun *et al.*, 2018). Further studies on candidate miRNA mutants or overexpressors would shed light on which are the main miRNAs that play a role on hypocotyl elongation during skotomorphogenesis.

Hook unfolding in darkness is transiently repressed by HYL1

A mutant allele of *HYL1* in Nossen ecotype (*hyl1-1*) was shown to display more open hooks than WT after 3 days in darkness (Lu and Fedoroff, 2000), but this finding was not further explored. The data presented here indicate that a proper hook unfolding response depends on the components of the microRNA pathway but, intriguingly, while HYL1 is necessary to repress it, SE and DCL1 perform an opposite role, promoting hook aperture. Our results also showed that the first dsRBD of HYL1 had a minor role in hook unfolding, as complementation of *hyl1-2* phenotypes in hook opening and adult leaves by *HYL1* mutants in this domain are clearly dissociated. Thus, it appears that HYL1 dsRBD2, the protein–protein interaction domain (Kurihara *et al.*, 2006; Qin *et al.*, 2010; Yang *et al.*, 2010; Machida *et al.*, 2011; Yang *et al.*, 2014), is the main driver of hook unfolding.

Our main hypothesis is that phosphorylated HYL1 represses hook unfolding in early skotomorphogenesis, peaking soon after seeds germinate to ensure protection of the meristem until seedlings reach the light. Some findings support this claim:

(i) Complementation of *hyl1-2* mutants with hyperphosphorylation mimics S42D and S159D results in hooks that are more closed than WT.

(ii) Only the phosphorylated pool of HYL1 can be detected in *se-1* and two alleles of *cpl1* mutants (Manavella *et al.*, 2012; Achkar *et al.*, 2018). These plants display the same phenotype, namely a more closed hook.

(iii) A recent report showed that HYL1 is mostly phosphorylated in darkness conditions including 4-days old dark-grown seedling (Achkar *et al.*, 2018).

(iv) Hyperphosphorylated HYL1 was detected in nucleoplasm but it was not found in dicing bodies (Manavella *et al.*, 2012).

Recently, Achkar and colleagues showed phosphorylated HYL1 is nuclear-localized and resistant to the degradation machinery (Achkar *et al.*, 2018). This strongly depends on its nucleus–cytoplasm shuttling through the balance of nuclear localization and export signal activities within the sequence of HYL1. In the light of the results presented here, nuclear-localized phosphorylated HYL1 appears to have a repressive role in hook unfolding. The specificity of phosphorylated HYL1 action during skotomorphogenesis is unexpected, as this population was suggested to be inactive during extended periods of light deprivation (Achkar *et al.*, 2018).

The independent action of HYL1 in hypocotyl elongation and hook unfolding might be related to its stability in the different tissues, as shown in Figure 1(e) and Table S1. HYL1 activity appears to vary between tissues, as suggested by our experiments on dissected samples. This can also be the reason for the relevance of CPL1 in hook unfolding, that contrasts with the minor role it plays in hypocotyl elongation. Recently, post-translational modification of HYL1 by CPL1 was shown to be affected by REGULATOR OF CBF GENE EXPRESSION 3 (RCF3) specifically in apex-enriched tissues (Karlsson *et al.*, 2015). We can envisage a similar scenario for hooks and hypocotyls during skotomorphogenesis although more work in specific cell-types is needed to produce a complete picture of this regulation.

Taken together, these results uncover an unprecedented role for HYL1 that is not linked to miRNA processing.

HYL1 action in skotomorphogenesis appears to be mediated by HY5 activity

HY5 is a master transcriptional regulator in the de-etiolation process of dark-grown seedlings to promote photomorphogenesis [revised in Gangappa and Botto (2016)]. As resources from the seeds should be well administrated until seedlings reach the light, HY5 activity must be completely shut-down in darkness to avoid triggering of useless biological processes. *HY5* mRNA was shown to be target of miR157d in light conditions (Tsai *et al.*, 2014), but our results suggest that this regulation is not taking place in darkness as expression analyses showed little or no differences in *HY5* expression levels in *hyl1-2* or *se-1* compared with WT. It was shown that unphosphorylated HY5,

the active form of this transcription factor, is ubiquitinated by COP1 in the nucleus and subject to proteasome-mediated degradation in darkness (Hardtke *et al.*, 2000; Osterlund *et al.*, 2000). Nevertheless, a small pool of phosphorylated HY5 protein, a form less physiologically active and more resistant to degradation, is still present in darkness (Hardtke *et al.*, 2000). This population was postulated to be necessary to quickly respond to illumination during the transition from dark to light (Hardtke *et al.*, 2000). Thus, the activity and stability of HY5 are regulated in opposite directions in darkness by its phosphorylation status. Our data clearly show that HY5 stability is compromised in *HYL1* mutants during skotomorphogenesis, but it appears to be active. One plausible explanation is that the phosphorylation status of HY5 might be shifted towards more active forms in *HYL1* mutants. Molecular and genetic data presented in this work support this hypothesis. First, we show that at least three direct targets of HY5 are overexpressed in dark-grown *hyl1-2* mutants. Second, epistasis analyses in double and single mutants of *HY5* and *HYL1* strongly suggest HYL1 negatively affects HY5 activity in darkness. *hyl1-2 hy5-2* double mutants showed a hook opening dynamics intermediate to single mutants or, in other terms, the absence of HY5 partially restored *hyl1-2* hook phenotype. The presence of an active population of HY5 acting in *hyl1-2* mutants could explain its partial photomorphogenic growth in darkness. Full complementation was not achieved in *hyl1-2 hy5-2* probably due to the presence of HY5 homolog (HYH). HYH shows functional redundancy with HY5 in other developmental processes such as hypocotyl growth, lateral root growth or pigment accumulation in light (revised in Gangappa and Botto, 2016). Also, the dynamics of complementation can be explained, as was suggested before, by a repressive role of phosphorylated HYL1 after seeds germinate that fades out during skotomorphogenesis. Further research will reveal if the role of HYL1 on HY5 activity is direct or if it is indirectly exerted by COP1.

In summary, this work provides evidence that the microprocessor adaptor HYL1 is required for important steps in seedling establishment during skotomorphogenesis in order to successfully develop from heterotrophic to autotrophic growth. Our results, together with recent findings (Manavella *et al.*, 2012; Achkar *et al.*, 2018), strongly suggest that HYL1 in its phosphorylated form have a role in hook development in darkness. We demonstrate that miRNA biogenesis is required for hypocotyl elongation in order to reach the light during skotomorphogenic growth as well. Finally, tight control of the activity and stability of HY5 in darkness could add a new layer of regulation mediated by HYL1, although further research is needed to elucidate whether this process is COP1 dependent or independent. Several questions have emerged from this study, which will be uncovered in the future by addressing the mechanism of this alternative role for HYL1 and how other HYL1-interacting factors influence its response.

EXPERIMENTAL PROCEDURES

Plant material and growth conditions

All mutants used in this work are in the Col-0 background. Mutant plants *hyl1-2* (SALK_064863), *se-1* (CS3257), *hst-15* (SALK_079290), *ago1-27* (Morel *et al.*, 2002), and *hen1-8* (Yu *et al.*, 2010) were obtained from Arabidopsis Biological Resource Center (ABRC) and have been described elsewhere (Prigge and Wagner, 2001; Morel *et al.*, 2002; Vazquez *et al.*, 2004). Transgenic lines p35S::HYL1 WT, p35S::HYL1 K17A/R19A (mR1), p35S::HYL1 Δ40-46 (mR2) and p35S::HYL1 R67A/K68A (mR3) in *hyl1-2* background were described elsewhere (Burdisso *et al.*, 2014). Transgenic lines pHYL1::HYL1 WT, pHYL1::HYL1 S42A, pHYL1::HYL1 S42D, pHYL1::HYL1 S159A, pHYL1::HYL1 S159D in *hyl1-2* background, *cpl1-3*, *cpl1-7* (Manavella *et al.*, 2012), and *dcl1-100* mutant lines (Laubinger *et al.*, 2010) were kindly provided by Dr Manavella. *hy5-2* (SALK_056405) mutant lines was a kind gift from Dr Martínez-García. pHY5::HY5-YFP *hy5* was kindly provided by Dr Botto. *hyl1-2 hy5-2* and *se-1 hy5-2* double mutants were obtained by crossing single homozygous mutants to obtain F2 progenies that were genotyped by PCR amplification of genomic DNA with specific primers (Table S3) as follows: hy5-2 gntyp F and hy5-2 gntyp R primers were used to amplify a band of ~250 bp corresponding to WT chromosome; LbB1 and hy5-2 gntyp were used to amplify a band of ~240 bp corresponding to the chromosome containing the *HY5* disruption by the T-DNA; se-1 gntyp F and se-1 gntyp R were used to amplify a band of 114 bp or 107 bp, corresponding to WT or the 7-bp deletion of *SE*-containing chromosomes, respectively. Purified bands from agarose gels were further digested with the restriction enzyme *Spe*I, which results in two fragments of 77 bp and 30 bp only for the *se-1* mutation. *hyl1-2* mutation was followed by selection on plates with 50 mg L^{-1} kanamycin due to the T-DNA insertion near the translation start site. pHY5::HY5-YFP *hy5-2 hyl1-2* were obtained by crossing pHY5::HY5-YFP *hy5* with *hyl1-2 hy5-2.* Genotyping of segregants were carried out as described above, where hy5-2 gntyp F and hy5-2 gntyp R primers were used to amplify a band of ~140 bp corresponding to pHY5::HY5-YFP construct. *hyl1-2 cpl1-3* and *hyl1-2 cpl1-7* double mutants were obtained by crossing single homozygous mutants to obtain F2 progenies that were genotyped by PCR amplification of genomic DNA with specific primers (Table S3) as follows: cpl1-3 gntyp F and cpl1-3 gntyp R primers were used to amplify a band of 341 bp. Purified bands from agarose gels were further digested with the restriction enzyme *Hin*dIII, which results in two fragments of 311 bp and 30 bp only for *cpl1-3* mutation; cpl1-7 gntyp F and cpl1-7 gntyp R primers were used to amplify a band of 102 bp. Purified bands from agarose gels were further digested with the restriction enzyme *Pst*I, which resulted in two fragments of 76 bp and 26 bp only for WT.

Plants in soil and seedlings in plates were grown in growth chambers in LD photoperiod (16 h light/8 h dark, ~100 μ mol m^{-2} sec^{-1}) or constant darkness at 22C.

Generation of transgenic lines

Plasmids containing pHYL1::HYL1-CFP and pSE::YFP-SE (Fang and Spector, 2007) used for transformation of *hyl1-2* or *se-1* plants, respectively, were a kind gift from Dr Fang and Dr Spector. *Agrobacterium tumefaciens* strain GV3101 containing each construct with the respective translational fusion under the

endogenous promoter were obtained and used to transform mutant plants by the floral dip method (Clough and Bent, 1998). Selection of each transgenic line in the following generations were performed as described (Fang and Spector, 2007).

Seedling growth and measurements

Seeds were surface sterilized for 2 min in 96% EtOH, transferred to 20% v/v NaOCl and 0.05% v/v Triton X-100 for 10 min, and rinsed five times with sterile distilled water. Seeds were then placed in Petri dishes containing half-strength (0.5) MS agar medium, covered with aluminium foil and stratified for 5 days in darkness at 4C. Only for experiments in Figure S2(c) we used Murashige and Skoog agar medium supplemented with 1% sucrose (MS1). Germination was induced with 3 h of white light in the growth chamber, plates were then covered with aluminium foil and placed inside a box, and incubated in the same growth chamber for the time points indicated in each experiment. For hypocotyl elongation and hook angle measurements, seedlings were arranged horizontally on a plate, photographed using a digital camera (Canon PowerShot SX50 HS) and measured with ImageJ 1.49k software. Hook angle was measured as the angle between the hypocotyl and an imaginary line between the cotyledons.

Experiments with *dcl1-100* seeds were carried out as described above, but arrangement of dark-grown seedlings on the plate and photographs were performed in sterile conditions in a hood. Plates were then incubated for an additional 4 days in LD and photographs were taken. Defective and normal seedlings (Figure S8b) were identified from the photographs of light-grown seedlings and used to mark and perform the measurements from the photographs of dark-grown seedlings. Segregation analysis was performed in order to confirm genotypes of mutant seedlings (Table S2).

Treatments with proteasome inhibitor were carried out as follow: after surface-sterilization, stratification, and light-induced germination, as described above, pHY5::HY5-YFP *hy5 hyl1-2* seeds were grown for 1 day in darkness on 0.5 MS plates and then transferred to 0.5 MS + 50 μM MG-132 (Cayman Chemical, Ann Arbor, MI, USA) or + DMSO as control for and additional 1 day in darkness. Treatments were initiated on 1 dD-grown seedlings because proteasome activity is required for germination of the seeds (Chiu *et al.*, 2016).

Dissection of samples

Seedlings grown in darkness for 2 days, as described above, were collected and flash-frozen in liquid N_2 and transitioned overnight to −20°C with RNA*later*®-ICE (Thermo Fisher Scientific, Ambion, Austin, TX, USA) as recommended by the manufacturer. Seedlings were transferred to a glass slide mounted on a platform with ice. Hooks and root tips were dissected with needles under a binocular microscope, collected and flash-frozen in microtubes. We used 100–150 seedlings for each genotype. Dissected tissue was kept at −70°C until extraction of RNA.

Confocal microscopy

Dark-grown seedlings of pHYL1::HYL1-CFP *hyl1-2* and pSE::YFP-SE *se-1*, at indicated times for each experiment, were transferred to glass slides, mounted in water and covered with a coverslip. Laser confocal microscopy was performed using a Plan Apochromat ×20, 0.8 NA lens on a Zeiss LSM880 microscope. Fluorescent fusion proteins were excited with the 458 nm (for CFP) and the 514 nm (for YFP) lines of an argon laser and fluorescence emission was collected from 459 to 522 nm (CFP) or 517 to 570 nm (YFP). Pictures were taken and fluorescence signal intensity of individual nucleus were analyzed using ImageJ 1.49k software. A region of interest (ROI) of approximately the size of a single nucleus was defined to standardize the measurements of nuclei between seedlings and samples. The 10 brightest nuclei from each seedling were chosen to obtain integrated density, and eight seedlings from each independent pHYL1::HYL1-CFP line were analyzed.

Gene expression analyses

Seedlings were grown in the dark, as described previously, for the indicated times for each experiment. ~100 mg of collected tissue, or 100–150 apical hooks or root tips from dissected samples, was used to extract total RNA by using the protocol described elsewhere (Piskurewicz and Lopez-Molina, 2011). Total RNA was then treated with DNase I RQ1 (Promega, Madison, WI, USA) according to the manufacturer's instructions. First-strand cDNA synthesis was performed using Moloney Murine Leukemia Virus (MMLV) reverse transcriptase (Invitrogen, Carlsbad, CA, USA), 2 μM oligo(dT) (dT25) and 2 μM random hexamers (Invitrogen) or 50 nM stem–loop specific primers (for miRNA expression analysis). cDNA obtained was then diluted to a final concentration of ~1 ng μl^{-1} with sterile distilled water. Real-time PCR was performed using 5 μl of cDNA, 300 nM each primer, *Taq* DNA polymerase (Genbiotech, Buenos Aires, Argentina) and EvaGreen™ as dye in the AriaMx Real-Time PCR System (Agilent, Santa Clara, CA, USA). miRNA levels were determined by stem–loop qPCR (Chen *et al.*, 2005), using specific forward primers for each miRNA and the reverse universal stem–loop primer (Universal SL R; Table S3). Each PCR was repeated at least two times, and the mean expression values from three technical replicates were used for further calculations. PP2AA3 was used as a normalization control as described previously (Shin *et al.*, 2007). Normalized gene expression is represented relative to the 2 days' dark-grown *hyl1-2* (in Figures 1f and S6a), *se-1* (in Figure 2e), and Col-0 (in Figures 1g, S5, S6b, 2f, and 5a–d) set at unity. Primer sequences for qRT-PCR can be found in Table S3.

Protein analyses

Total proteins were extracted using urea buffer: 50 mM Tris–HCl (pH 7.5), 4 M urea, 150 mM NaCl, 0.1 % NP-40, Protease inhibitor mix (Merck), and 50 μM MG-132 (Cayman Chemical). Protein extracts were separated by 12% SDS-PAGE, transferred to nitrocellulose membrane (Amersham, Piscataway, NJ, USA), immunoblotted with a 1:1000 dilution of α-HY5 primary antibody (Agrisera, Vännäs, Sweden) and a 1:10 000 dilution of α-rabbit IgG HRP-conjugated secondary antibody (Agrisera). Chemiluminescence detection was performed using Hyperfilm ECL (Amersham). Ponceau staining was used as loading control.

Statistical analyses

Data were analyzed using Student's *t*-test when two sample datasets were compared or one-way ANOVA for more than two datasets, and the differences between means were evaluated using Tukey's post-test (Infostat Software v.2017, Facultad de Ciencias Agropecuarias, Universidad Nacional de Córdoba, Córdoba, Argentina). Statistically significant differences were defined as those with a *P-value* <0.05 or <0.01, as indicated.

ACCESSION NUMBERS

HYL1 (At1g09700), SE (At2g27100), DCL1 (At1g01040), CPL1 (At4g21670), HST (At3g05040), HEN1 (At4g20910),

AGO1 (At1g48410), HY5 (At5g11260), PIF3 (At1g09530), RBCS1A (At1g67090), CHS (At5g13930), PIL1 (At2g46970), XTR7 (At4g14130), CAB1 (At1g29930), MIR156b (At4g30972), MIR156c (At4g31877), MIR156d (At5g10945), MIR159b (At1g18075), MIR162a (At5g08185), MIR164c (At5g27807), MIR166a (At2g46685), MIR166b (At3g61897), MIR171b (At1g11735), PP2AA3 (At1g13320).

ACKNOWLEDGEMENTS

We thank Diego Aguirre for plant care in growth chambers; Rodrigo Vena for technical assistance with confocal microscopy; Pablo Manavella for *cpl1-3*, *cpl1-7*, *dcl1-100*, and HYL1 phosphomimics seeds; Jaume Martínez-García for *hy5-2* seeds; Javier Botto for pHY5::HY5-YFP *hy5* seeds; Yuda Fang and David L. Spector for plasmids containing pHYL1::HYL1-CFP and pSE::YFP-SE.

AUTHOR CONTRIBUTIONS

JMS, RC, and NG-S performed the experiments; JMS and NG-S analyzed the data; NG-S conceived the project and wrote the manuscript; RR, JP, and NG-S provided the funding and revised the manuscript. All authors read and approved the final manuscript.

CONFLICT OF INTEREST

The authors declare that they have no competing interests.

FUNDING

This research was funded by Agencia Nacional de Promoción Científica y Tecnológica (PICT2013-3281 and PICT2016-0314).

SUPPORTING INFORMATION

Additional Supporting Information may be found in the online version of this article.

Figure S1. *hyl1-2* mutants do not show a delay in germination. One-day dark-grown control (Col-0) and *hyl1-2* seedlings in 0.5 MS agarose plates.

Figure S2. Hypocotyl elongation in light-grown *hyl1-2* mutants. (a) Representative *hyl1-2* and control (Col-0) seedlings grown for 3 days in long day (LD, 16 h light/8 h dark) are shown. (b) Hypocotyl length of *hyl1-2* and Col-0 light-grown seedlings on half-strength MS (0.5 MS) at the indicated time points. (c) Hypocotyl length of *hyl1-2* and Col-0 4-days light-grown seedlings in 0.5 MS or MS supplemented with 1% sucrose (MS1). dLD indicates days in LD. Data are presented as mean ± SEM of at least 40 seedlings from two biological replicas. Bar in (a) represents 2 mm.

Figure S3. Characterization of transgenic lines that express HYL1-CFP. (a) Integrated fluorescence intensity of root nuclei from 2-days dark-grown pHYL1::HYL1-CFP *hyl1-2* seedlings. Data are presented as mean ± SEM of at least 60 nuclei from two biological replicas. AU, Arbitrary units. Statistically significant differences between groups are indicated by different letters (ANOVA, $P < 0.05$). (b) Representative confocal fluorescence images of roots from 2-days dark-grown pHYL1::HYL1-CFP *hyl1-2* seedlings. (c) Hypocotyl length and (d) hook angle measurements of *hyl1-2*, Col-0 and pHYL1::HYL1-CFP *hyl1-2* dark-grown seedlings at the indicated time points. Data are presented as mean ± SEM of at least 40 seedlings from two biological replicas. (e) pHYL1::HYL1-CFP *hyl1-2* and control plants grown for 15 days in long day (LD).

Figure S4. HYL1-CFP displays two different localization patterns in darkness. Confocal fluorescence images of roots from 3-days dark-grown pHYL1::HYL1-CFP *hyl1-2* seedlings. (a) Discrete nuclear and (b) diffuse localization patterns of fluorescence.

Figure S5. Expression levels of pri-miRNAs in dark-grown *hyl1-2* and *se-1* mutants. qRT-PCR analysis of *hyl1-2*, *se-1*, and Col-0 dark-grown seedlings at the indicated time points. dD, days in darkness. Expression levels of miRNA precursors were normalized to *PP2AA3* housekeeping gene and expressed relative to the Col-0 2 dD value set at unity. Means ± SEM are shown from technical triplicates and two biological replicas. Asterisks indicate statistically different mean values compared with their corresponding wild-type ($P < 0.05$).

Figure S6. Expression levels of miRNAs and pri-miRNAs in dissected tissues from dark-grown *hyl1-2* mutants. qRT-PCR (a) and stem–loop qRT-PCR (b) analysis, respectively, of dissected tissue from *hyl1-2* and Col-0 2-days dark-grown seedlings. Between 100 and 150 seedlings were used to dissect root tips and apical hooks for each sample. Expression levels of pri-miRNA (a) or miRNAs (b) were normalized to the *PP2AA3* housekeeping gene and expressed relative to the *hyl1-2* (a) or Col-0 (b) roots value set at unity. Means ± SEM are shown from technical triplicates and two biological replicas. Asterisks indicate statistically different mean values compared with their corresponding wild-type ($P < 0.05$).

Figure S7. Hypocotyl elongation in light-grown *se-1* mutants. (a) Representative *se-1* and control (Col-0) seedlings grown for 3 days in long day (LD, 16 h light/8 h dark). (b) Hypocotyl length of *se-1* and Col-0 light-grown seedlings at the indicated time points. dLD indicates days in LD. Data are presented as mean ± SEM of at least 40 seedlings from two biological replicas. Bar in (a) = 2 mm.

Figure S8. DCL1 is required for skotomorphogenesis. Representative homozygous (*dcl1-100*) and heterozygous (*dcl1-100*/+) or control seedlings from a *dcl1-100*/+ segregating population, and control siblings (WT) grown in (a) darkness for 3 days (3 dD), (b) plus 4 days under long day conditions (3 dD + 4 dLD). (c) Hypocotyl length and (d) hook angle measurements of *dcl1-100* and control dark-grown seedlings at the indicated time points. Data are presented as mean ± SEM of at least 10 seedlings from two biological replicas. Asterisks in (c) and (d) indicate statistically different mean values compared with their corresponding wild-type ($P < 0.05$). Bars in (a) and (b) represent 5 mm.

Figure S9. Hook phenotypes in mutants of miRNA pathway. (a) hook angle measurements of *ago1-27*, *hst-15*, *hen1-8*, and control dark-grown seedlings at the indicated time points. dD indicates days in the dark. Data are presented as mean ± SEM of at least 15 seedlings from two biological replicas. Asterisks indicate statistically different mean values compared with their corresponding wild-type in both biological replicas ($P < 0.05$). (b) wild-type (Col-0) and mutant plants from (a) grown for 22 days under long day (LD) conditions.

Figure S10. Complementation of *hyl1-2* defects in leaves by dsRBD1 mutant versions of HYL1. p35S::HYL1 *hyl1-2* comprising mR1 (K17A/R19A), mR2 (Δ40-46), mR3 (R67A/K68A) and wild-type (WT) mutant versions of dsRBD1, and control plants grown for 15 days under long day (LD) conditions.

Figure S11. Phenotypes in leaves of *CPL1* mutant adult plants. Mild (*cpl1-3*) and strong (*cpl1-7*) mutant alleles of *CPL1*, *hyl1-2* and control plants grown for 18 days under long day (LD) conditions.

Figure S12. Epistasis analysis in *hyl1-2* and *cpl1* double mutants. (a) Hypocotyl length and (b) hook angle measurements of Col-0,

hyl1-2, *cpl1-3*, and double mutants *hyl1-2 cpl1-3* dark-grown seedlings at the indicated time points. (c) and (d) Representative hooks of 2- and 4-days, respectively, dark-grown mutant lines from (b). (e) Hypocotyl length and (f) hook angle measurements of Col-0, *hyl1-2*, *cpl1-7*, and double mutants *hyl1-2 cpl1-7* dark-grown seedlings at the indicated time points. (g) and (h) Representative hooks of 2- and 4-days, respectively, dark-grown mutant lines from (f). dD, days in darkness. Data are presented as means ± SEM of at least 40 seedlings from two biological replicas. Statistically significant differences between groups are indicated by different letters (ANOVA, $P < 0.05$).

Figure S13. Complementation of *hyl1-2* defects in leaves by HYL1 phosphorylation mimics. pHYL1::HYL1 *hyl1-2* comprising hypophosphorylation mimics (S42A and S159A), hyperphosphorylation mimics (S42D and S159D), or wild-type (WT) version of HYL1, and control plants grown for 18 days in long day (LD).

Figure S14. HY5 accumulation in dark-grown *hyl1-2* background depends on the proteasome. α-HY5 western blots of 2-days dark-grown pHY5::HY5-YFP *hy5-2 hyl1-2* seedlings treated with the proteasome inhibitor MG-132. After light induction seeds were germinated in 0.5 MS for 1 day in darkness and then transferred for one more day in darkness either with 0.5 MS +MG-132 50 μM (MG) or +DMSO as control (Mock). Ponceau stainings were used as loading controls.

Figure S15. Expression analyses of *HY5* in HY5-YFP lines. *HY5* expression levels in 4-days dark-grown pHY5::HY5-YFP *hy5-2* (HY5-YFP) and pHY5::HY5-YFP *hyl1-2 hy5-2* (HY5-YFP hyl1-2) were measured by qRT-PCR. Expression levels were normalized to *PP2AA3* housekeeping gene and expressed relative to the HY5-YFP value. Means ± SEM are shown from technical duplicates.

Table S1. Localization patterns of HYL1-CFP during skotomorphogenesis.

Table S2. Segregation analysis of *dcl1-100* heterozygous seedlings.

Table S3. Primers used in this work.

REFERENCES

Achkar, N.P., Cho, S.K., Poulsen, C. *et al.* (2018) A quick HYL1-dependent reactivation of MicroRNA production is required for a proper developmental response after extended periods of light deprivation. *Dev. Cell*, **46**, 236–247.e6.

Baumberger, N. and Baulcombe, D.C. (2005) Arabidopsis ARGONAUTE1 is an RNA Slicer that selectively recruits microRNAs and short interfering RNAs. *Proc. Natl. Acad. Sci. USA*, **102**, 11928–11933.

Bollman, K.M., Aukerman, M.J., Park, M.Y., Hunter, C., Berardini, T.Z. and Poethig, R.S. (2003) HASTY, the Arabidopsis ortholog of exportin 5/MSN5, regulates phase change and morphogenesis. *Development*, **130**, 1493–1504.

Burdisso, P., Milia, F., Schapire, A.L., Bologna, N.G., Palatnik, J.F. and Rasia, R.M. (2014) Structural determinants of Arabidopsis thaliana Hyponastic leaves 1 function in vivo. *PLoS ONE*, **9**, e113243.

Chattopadhyay, S., Ang, L.H., Puente, P., Deng, X.W. and Wei, N. (1998) Arabidopsis bZIP protein HY5 directly interacts with light-responsive promoters in mediating light control of gene expression. *Plant Cell*, **10**, 673–683.

Chen, C., Ridzon, D.A., Broomer, A.J. *et al.* (2005) Real-time quantification of microRNAs by stem-loop RT-PCR. *Nucleic Acids Res.* **33**, e179.

Chiu, R.S., Pan, S., Zhao, R. and Gazzarrini, S. (2016) ABA-dependent inhibition of the ubiquitin proteasome system during germination at high temperature in Arabidopsis. *Plant J*, **88**, 749–761.

Cho, S.K., Ben Chaabane, S., Shah, P., Poulsen, C.P. and Yang, S.W. (2014) COP1 E3 ligase protects HYL1 to retain microRNA biogenesis. *Nat. Commun.* **5**, 5867.

Clough, S.J. and Bent, A.F. (1998) Floral dip: a simplified method for Agrobacterium-mediated transformation of Arabidopsis thaliana. *Plant J.* **16**, 735–43.

Dong, Z., Han, M.H. and Fedoroff, N. (2008) The RNA-binding proteins HYL1 and SE promote accurate in vitro processing of pri-miRNA by DCL1. *Proc. Natl. Acad. Sci. USA*, **105**, 9970–9975.

Fang, Y. and Spector, D.L. (2007) Identification of nuclear dicing bodies containing proteins for microRNA biogenesis in living Arabidopsis plants. *Curr. Biol.* **17**, 818–823.

Gangappa, S.N. and Botto, J.F. (2016) The Multifaceted roles of HY5 in plant growth and development. *Mol. Plant*, **9**, 1353–1365.

Gommers, C.M.M. and Monte, E. (2018) Seedling establishment: a dimmer switch-regulated process between dark and light signaling. *Plant Physiol.* **176**, 1061–1074.

Hardtke, C.S., Gohda, K., Osterlund, M.T., Oyama, T., Okada, K. and Deng, X.W. (2000) HY5 stability and activity in arabidopsis is regulated by phosphorylation in its COP1 binding domain. *EMBO J.* **19**, 4997–5006.

Iwata, Y., Takahashi, M., Fedoroff, N.V. and Hamdan, S.M. (2013) Dissecting the interactions of SERRATE with RNA and DICER-LIKE 1 in Arabidopsis microRNA precursor processing. *Nucleic Acids Res.* **41**, 9129–9140.

Josse, E.M. and Halliday, K.J. (2008) Skotomorphogenesis: the dark side of light signalling. *Curr. Biol.* **18**, R1144–R1146.

Karlsson, P., Christie, M.D., Seymour, D.K., Wang, H., Wang, X., Hagmann, J., Kulcheski, F. and Manavella, P.A. (2015) KH domain protein RCF3 is a tissue-biased regulator of the plant miRNA biogenesis cofactor HYL1. *Proc. Natl. Acad. Sci. USA*, **112**, 14096–14101.

Kurihara, Y., Takashi, Y. and Watanabe, Y. (2006) The interaction between DCL1 and HYL1 is important for efficient and precise processing of pri-miRNA in plant microRNA biogenesis. *RNA*, **12**, 206–212.

Laubinger, S., Zeller, G., Henz, S.R., Buechel, S., Sachsenberg, T., Wang, J.W., Ratsch, G. and Weigel, D. (2010) Global effects of the small RNA biogenesis machinery on the Arabidopsis thaliana transcriptome. *Proc. Natl. Acad. Sci. USA*, **107**, 17466–17473.

Lee, J., He, K., Stolc, V., Lee, H., Figueroa, P., Gao, Y., Tongprasit, W., Zhao, H., Lee, I. and Deng, X.W. (2007) Analysis of transcription factor HY5 genomic binding sites revealed its hierarchical role in light regulation of development. *Plant Cell*, **19**, 731–749.

Leivar, P., Monte, E., Oka, Y., Liu, T., Carle, C., Castillon, A., Huq, E. and Quail, P.H. (2008) Multiple phytochrome-interacting bHLH transcription factors repress premature seedling photomorphogenesis in darkness. *Curr. Biol.* **18**, 1815–1823.

Leivar, P., Tepperman, J.M., Monte, E., Calderon, R.H., Liu, T.L. and Quail, P.H. (2009) Definition of early transcriptional circuitry involved in light-induced reversal of PIF-imposed repression of photomorphogenesis in young Arabidopsis seedlings. *Plant Cell*, **21**, 3535–3553.

Lorrain, S., Trevisan, M., Pradervand, S. and Fankhauser, C. (2009) Phytochrome interacting factors 4 and 5 redundantly limit seedling de-etiolation in continuous far-red light. *Plant J.* **60**, 449–461.

Lu, C. and Fedoroff, N. (2000) A mutation in the Arabidopsis HYL1 gene encoding a dsRNA binding protein affects responses to abscisic acid, auxin, and cytokinin. *Plant Cell*, **12**, 2351–2366.

Machida, S., Chen, H.Y. and Adam Yuan, Y. (2011) Molecular insights into miRNA processing by Arabidopsis thaliana SERRATE. *Nucleic Acids Res.* **39**, 7828–7836.

Manavella, P.A., Hagmann, J., Ott, F., Laubinger, S., Franz, M., Macek, B. and Weigel, D. (2012) Fast-forward genetics identifies plant CPL phosphatases as regulators of miRNA processing factor HYL1. *Cell*, **151**, 859–870.

Mazzella, M.A., Casal, J.J., Muschietti, J.P. and Fox, A.R. (2014) Hormonal networks involved in apical hook development in darkness and their response to light. *Front. Plant Sci.* **5**, 52.

Morel, J.B., Godon, C., Mourrain, P., Beclin, C., Boutet, S., Feuerbach, F., Proux, F. and Vaucheret, H. (2002) Fertile hypomorphic ARGONAUTE (ago1) mutants impaired in post-transcriptional gene silencing and virus resistance. *Plant Cell*, **14**, 629–639.

Osterlund, M.T., Hardtke, C.S., Wei, N. and Deng, X.W. (2000) Targeted destabilization of HY5 during light-regulated development of Arabidopsis. *Nature*, **405**, 462–466.

Park, M.Y., Wu, G., Gonzalez-Sulser, A., Vaucheret, H. and Poethig, R.S. (2005) Nuclear processing and export of microRNAs in Arabidopsis. *Proc. Natl. Acad. Sci. USA*, **102**, 3691–3696.

Piskurewicz, U. and Lopez-Molina, L. (2011) Isolation of genetic material from Arabidopsis seeds. *Methods Mol. Biol.* **773**, 151–164.

Prigge, M.J. and Wagner, D.R. (2001) The arabidopsis serrate gene encodes a zinc-finger protein required for normal shoot development. *Plant Cell*, **13**, 1263–1279.

Qin, H., Chen, F., Huan, X., Machida, S., Song, J. and Yuan, Y.A. (2010) Structure of the Arabidopsis thaliana DCL4 DUF283 domain reveals a noncanonical double-stranded RNA-binding fold for protein-protein interaction. *RNA*, **16**, 474–481.

Raghuram, B., Sheikh, A.H., Rustagi, Y. and Sinha, A.K. (2015) MicroRNA biogenesis factor DRB1 is a phosphorylation target of mitogen activated protein kinase MPK3 in both rice and Arabidopsis. *FEBS J.* **282**, 521–536.

Rasia, R.M., Mateos, J., Bologna, N.G., Burdisso, P., Imbert, L., Palatnik, J.F. and Boisbouvier, J. (2010) Structure and RNA interactions of the plant MicroRNA processing-associated protein HYL1. *Biochemistry*, **49**, 8237–8239.

Schauer, S.E., Jacobsen, S.E., Meinke, D.W. and Ray, A. (2002) DICER-LIKE1: blind men and elephants in Arabidopsis development. *Trends Plant Sci.* **7**, 487–491.

Shin, J., Park, E. and Choi, G. (2007) PIF3 regulates anthocyanin biosynthesis in an HY5-dependent manner with both factors directly binding anthocyanin biosynthetic gene promoters in Arabidopsis. *Plant J.* **49**, 981–994.

Su, C., Li, Z., Cheng, J., Li, L., Zhong, S., Liu, L., Zheng, Y. and Zheng, B. (2017) The protein phosphatase 4 and SMEK1 complex dephosphorylates HYL1 to promote miRNA biogenesis by antagonizing the MAPK cascade in Arabidopsis. *Dev. Cell*, **41**, 527–539.e5.

Sun, Z., Li, M., Zhou, Y., Guo, T., Liu, Y., Zhang, H. and Fang, Y. (2018) Coordinated regulation of Arabidopsis microRNA biogenesis and red light signaling through Dicer-like 1 and phytochrome-interacting factor 4. *PLoS Genet.* **14**, e1007247.

Tsai, H.L., Li, Y.H., Hsieh, W.P., Lin, M.C., Ahn, J.H. and Wu, S.H. (2014) HUA ENHANCER1 is involved in posttranscriptional regulation of positive and negative regulators in Arabidopsis photomorphogenesis. *Plant Cell*, **26**, 2858–2872.

Vazquez, F., Gasciolli, V., Crete, P. and Vaucheret, H. (2004) The nuclear dsRNA binding protein HYL1 is required for microRNA accumulation and plant development, but not posttranscriptional transgene silencing. *Curr. Biol.* **14**, 346–351.

Wang, Z., Ma, Z., Castillo-Gonzalez, C., Sun, D., Li, Y., Yu, B., Zhao, B., Li, P. and Zhang, X. (2018) SWI2/SNF2 ATPase CHR2 remodels pri-miRNAs via Serrate to impede miRNA production. *Nature*, **557**, 516–521.

Wu, F., Yu, L., Cao, W., Mao, Y., Liu, Z. and He, Y. (2007) The N-terminal double-stranded RNA binding domains of Arabidopsis HYPONASTIC LEAVES1 are sufficient for pre-microRNA processing. *Plant Cell*, **19**, 914–925.

Yan, J., Wang, P., Wang, B. *et al.* (2017) The SnRK2 kinases modulate miRNA accumulation in Arabidopsis. *PLoS Genet.* **13**, e1006753.

Yang, L., Liu, Z., Lu, F., Dong, A. and Huang, H. (2006) SERRATE is a novel nuclear regulator in primary microRNA processing in Arabidopsis. *Plant J.* **47**, 841–850.

Yang, S.W., Chen, H.Y., Yang, J., Machida, S., Chua, N.H. and Yuan, Y.A. (2010) Structure of Arabidopsis HYPONASTIC LEAVES1 and its molecular implications for miRNA processing. *Structure*, **18**, 594–605.

Yang, X., Ren, W., Zhao, Q., Zhang, P., Wu, F. and He, Y. (2014) Homodimerization of HYL1 ensures the correct selection of cleavage sites in primary miRNA. *Nucleic Acids Res.* **42**, 12224–12236.

Yu, B., Yang, Z., Li, J., Minakhina, S., Yang, M., Padgett, R.W., Steward, R. and Chen, X. (2005) Methylation as a crucial step in plant microRNA biogenesis. *Science*, **307**, 932–935.

Yu, B., Bi, L., Zhai, J., Agarwal, M., Li, S., Wu, Q., Ding, S.W., Meyers, B.C., Vaucheret, H. and Chen, X. (2010) siRNAs compete with miRNAs for methylation by HEN1 in Arabidopsis. *Nucleic Acids Res.* **38**, 5844–5850.

